18th Brazilian Congress of Thermal Sciences and Engineering
November 16-20, 2020 (Online)

ENC-2020-0035
NUMERICAL ANALYSIS OF THE NATURAL CONVECTIVE HEAT TRANSFER BETWEEN TWO HORIZONTAL ISOTHERMAL WAVY SURFACES

William Nunes
Santiago del Rio Oliveira
Department of Mechanical Engineering, São Paulo State University, 14-01 Engenheiro Luiz Edmundo Carrijo Coube Avenue, Bauru, SP, 17033-360, Brazil.
w.nunes@unesp.br, santiago.oliveira@unesp.br

Abstract. *This work consists of the numerical analysis of the natural convective heat transfer from two horizontal surfaces separated vertically containing waves on both sides. The vertical distance that separates the surfaces is relatively small in such a way that the flow from both surfaces influences the heat transfer rates from each surface. The waves considered in this work have a rectangular shape with constant height, having the effect of increasing the heat transfer rate of the heated plates to an adjacent fluid, in this case, ambient air. The main objective of this article is to determine the natural convective heat transfer rates from the horizontal wavy surfaces to the ambient air. Effects on the natural convective heat transfer from the individual surfaces of each plate as well as from the total surface of each plate will be analyzed according to the following variables: dimensionless height of the waves, dimensionless vertical distance between the surfaces and the Rayleigh number. Results will be obtained numerically using the standard* $k-\varepsilon$ *turbulence model including effects of buoyant forces with the aid of the commercial CFD solver ANSYS FLUENT©. Depending on the results obtained, geometric recommendations of the situation under analysis can be made that provide the greatest improvement in the natural convective heat transfer rate from the horizontal wavy surfaces.*

Keywords: *natural convective heat transfer, wavy surfaces, heat transfer enhancement,* $k-\varepsilon$ *turbulence model*

1. INTRODUCTION

Natural convective heat transfer occurs in many practical situations and remains an area of considerable basic and applied interest. In the present article attention will be restricted to external natural convective flows, that is, flow situations in which there are no constraining surfaces near enough to the surface considered or that have any significant influence on the natural convective flow over this surface. Increasing the heat transfer rate in a given situation involving natural convective flows is often difficult to accomplish, one method of attempting to enhance natural convective heat transfer rates is use surfaces that have a wavy surface.

The enhancement of the heat transfer rate produced by using a wavy surface arises from the increase in the surface area exposed to the fluid to which the heat is being transferred and, in some cases, to the changes in the near surface flow produced by the presence of the surface waves. The total enhancement of the heat transfer rate will depend on the shape and relative size of the surface waves. Many wavy shapes have been considered in past studies but the most common shapes considered remain rectangular, triangular and sinusoidal waves. The enhancement of the heat transfer rate produced by using a wavy surface will also depend on the flow situation being considered, for example, flow over a plane surface or cylindrical surface and on the thermal boundary conditions at the surface. The two surface boundary conditions most commonly considered are those in which there is a temperature or a uniform heat flux over the surface, another factor that influences the natural convective heat transfer rate from a surface is its orientation, that is, is it horizontal, is it vertical or is it inclined and whether, when inclined, it is facing upward or downward (Oosthuizen, 2016).

While there have been some limited previous studies of natural convective heat transfer from thin, two-sided horizontal plates, these studies have mainly considered only the case where the plate is flat (non-wavy) and where the flow over the plates is laminar. Here, the conditions considered are such that laminar flow, transitional flow, and turbulent flow can occur over the plate. Numerical studies of heat transfer from a horizontal surface having rectangular waves and triangular waves for conditions under which laminar, transitional, and turbulent flow exist are described in (Oosthuizen, 2016a) and (Oosthuizen, 2016b). Other studies of natural convective heat transfer from horizontal wavy surfaces are described in (Prétot *et al*., 2000), (Prétot *et al*., 2003), (Siddiqa and Hossain, 2013) and (Siddiqa *et al*., 2015). In all of these studies, the natural convective heat transfer rate was obtained from a thin, one-sided, two-dimensional horizontal wavy plate having a uniform surface temperature. Studies of natural convective heat transfer from a one thin, two-sided, two-dimensional wavy plate having a uniform surface temperature are described in (Oliveira and Oosthuizen, 2018) and (Oliveira and Oosthuizen, 2019). However, studies of natural convective heat transfer from two thin, two-sided, two-dimensional wavy plates having a uniform surface temperature, have not yet been made.

The purpose of the present article is to undertake a numerical study of natural convective heat transfer from a thin, two-sided, two-dimensional horizontal two plates having a uniform surface temperature and thus be able to understand how the heat flow behaves with the different wave dimensions and spacing between the plates above and below and check if this flow interacts between the plates. The surface shape is wavy, and attention has been given to the case where the surface waves have a rectangular shape with constant height. The importance of the present work is related to the increase of the natural convective heat transfer rate in situations where the implementation of forced convection would be difficult to apply or even impossible and thus present a numerical analysis that helps to define the best dimensions for the wavy surfaces and provides the best heat transfer by natural convection. This may be the case, for example, when cooling a circuit board assembly or in cases where the thermal management of electronic components must be performed in more detail.

2. PHYSICAL SITUATION

The physical situation analyzed in this work can be visualized in **Figure 1**:

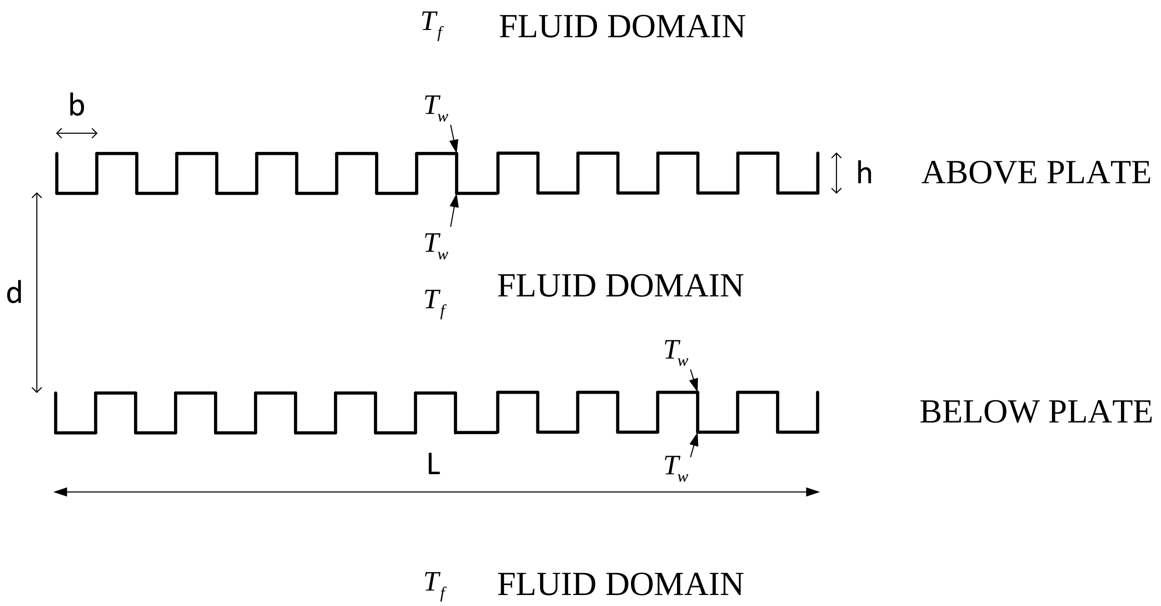

Figure 1. Two horizontal wavy surfaces.

The situation under analysis consists of two thin, two-sided, two-dimensional horizontal plates having a uniform surface temperature T_w. The surface shape of both plates are wavy and attention has been given to the case where the surface have nineteen rectangular waves on both plates and these waves are equally spaced with constant width b. The plates are in contact with a surrounding fluid at constant temperature T_f. For a heated surface, $T_w > T_f$ and both the top and bottom surfaces of both plates will exchange energy with the surrounding fluid by natural convection. The horizontal surfaces have unit width *L*, unit depth *w* and the vertical distance between plates is denoted by d. The purpose of this study is to calculate the heat transfer rate by natural convection between the heated surfaces and the surrounding fluid. The Nusselt numbers are different between top/bottom parts of each plates, thus, the results were presented as mean Nusselt numbers, where these results are related to the natural convective heat transfer from the top and bottom surfaces of each plate. Thus, these results were calculated using the Newton's law of cooling and the definition of the mean Nusselt number based on the vertical distance between the surfaces, i.e.:

$$\overline{\mathrm{Nu}}_{d\ (\mathrm{above,top/bottom})} = \frac{q_{(\mathrm{above,top/bottom})}d}{A(T_w - T_f)k} \tag{1}$$

$$\overline{\mathrm{Nu}}_{d\ (\mathrm{below,top/bottom})} = \frac{q_{(\mathrm{below,top/bottom})}d}{A(T_w - T_f)k} \tag{2}$$

Where $\overline{\mathrm{Nu}}_d$ is the mean Nusselt number based on *d* and on the mean heat transfer rate, q is the mean heat transfer rate, k is the thermal conductivity of the fluid and *A* is the heat transfer area, calculated using *L*, *b*, *h* and the number of waves, according to Fig. 1.

3. SOLUTION PROCEDURE

In obtaining the numerical results discussed above the mean flow has been assumed to be steady, the Boussinesq approximation has been used, i.e., fluid properties have been assumed to be constant except for the density change with temperature in momentum equation, where this gives rise to the buoyancy forces and the density change being assumed to be proportional to the temperature change. Radiant heat transfer effects have been neglected and allowance has been made for the possibility that turbulent flow can occur in the system with the increase of heat flow. Thus, in order to deal with this, the standard $k-\varepsilon$ turbulence model with standard wall functions and with full account being taken of buoyancy force effects has been used to adapt the model and better represent the system.

The mathematical model consists of an equation for the turbulent kinetic energy κ, Eq. (3), and a transport equation for the dissipation of turbulent kinetic energy ε, Eq. (4):

$$\frac{\partial(\rho\kappa)}{\partial t} + \mathrm{div}\,(\rho\kappa \mathrm{U}) = \mathrm{div}\left[\frac{\mu_t}{\sigma_\kappa}\ \mathrm{grad}\ \kappa\right] + 2\mu_t S_{ij}\cdot S_{ij} - \rho\varepsilon \tag{3}$$

$$\frac{\partial(\rho\varepsilon)}{\partial t} + \mathrm{div}\,(\rho\varepsilon \mathrm{U}) = \mathrm{div}\left[\frac{\mu_t}{\sigma_\varepsilon}\ \mathrm{grad}\ \varepsilon\right] + C_{1\varepsilon}\frac{\varepsilon}{\kappa}2\mu_t S_{ij}\cdot S_{ij} - C_{2\varepsilon}\rho\frac{\varepsilon^2}{\kappa} \tag{4}$$

Equations (3) and (4) contains five adjustable constants, e.g., C_μ, σ_k, σ_ε, $C_{1\varepsilon}$ and $C_{2\varepsilon}$. The standard $k-\varepsilon$ turbulence model uses values for these constants obtained through comprehensive curve adjustments for a wide range of turbulent flows, i.e., $C_\mu = 0.09$, $\sigma_k = 1.00$, $\sigma_\varepsilon = 1.30$, $C_{1\varepsilon} = 1.44$ and $C_{2\varepsilon} = 1.92$. U is the velocity vector, μ_t is the turbulent viscosity and S_{ij} is the deformation rate. The horizontal wavy surfaces has unit depth w and unit width *L* maintained at a uniform surface temperature $T_w = 310$ K. The surrounding fluid is air at a temperature $T_f = 290$ K at atmospheric pressure in all cases.

The governing equations subject to the boundary conditions have been solved numerically using the commercial CFD solver ANSYS FLUENT©. The numerical approach used here in order to determine when turbulence develops which involves solving the Reynolds averaged governing equations together with a turbulence model, in which the effects of buoyancy forces are taken into account for all conditions considered and then monitoring the results obtained with increasing Rayleigh numbers to determine when significant turbulence effects develop. This approach has been used quite extensively in the study of forced convective flows, e.g., see (Schmidt and Patankar, 1991) and (Zheng *et al.*, 1998). The solutions presented in this work all basically have the following parameters:

1. The Rayleigh number, Ra_d, based on the reference length scale d, that is the vertical distance that separate the horizontal heated surfaces and the difference between the temperature of the heated surfaces, T_w, and the temperature of the undisturbed fluid well away from the system, T_f, i.e.:

$$Ra_d = \frac{g\beta(T_w - T_f)d^3}{\nu\alpha} \tag{5}$$

2. The dimensionless width of the waves, $B = b/L$;
4. The dimensionless height of the waves, $H = h/L$;
5. The dimensionless vertical distance between the plates, $D = d/L$ and
5. The Prandtl number, Pr.

In Eq. (5), Ra_d is the Rayleigh number based on *d*, *g* is the gravitational acceleration, β is the bulk coefficient of thermal expansion, *d* is the vertical distance between the plates, ν is the kinematic viscosity of the fluid and α is the thermal diffusivity of the fluid. Results have only been obtained for a Prandtl number of 0.71, i.e., effectively the value for air at 300 K. Before obtaining numerical results, a mesh independence study was carried out using the highest Rayleigh number value, i.e., 10^{12}, for a case where $B = H = 0.0526232$ and $D = 0.1$. All meshes were created with the aid of the GAMBIT© software. Results of the mesh independence test can be seen in Tab. 1:

Table 1. Mesh independence test

Number of elements	$\overline{\mathrm{Nu}}_{d\ (\mathrm{above,total})}$	$\overline{\mathrm{Nu}}_{d\ (\mathrm{below,total})}$
106.200	15.809	13.584
152.928	16.542	14.225
208.152	17.854	14.987
271.872	18.789	15.654
344.088	19.541	15.789
424.800	19.874	15.923
514.008	19.645	15.811

According to Tab. 1, for 424.800 elements, the mean Nusselt numbers remained approximately constant. This number of elements was then used in all numerical simulations. In all simulations, the mean Nusselt number integrated over the surface was monitored to ensure convergence and to verify that the simulation reached the steady state. The complete computational domain is 2.5m width and 3.5m high. Due to symmetry, half of the computational domain was simulated. The configuration of the ANSYS FLUENT© solver was based on the work of Oliveira and Oosthuizen (2018), Oliveira and Oosthuizen (2019), Oosthuizen (2016a) and Oosthuizen (2016b), having already been extensively tested and validated with results of numerical and experimental works by these authors. The convergence criteria used for all variables in numerical simulations was 10^{-5}. Figure 2 show an excerpt of the mesh used in numerical simulations:

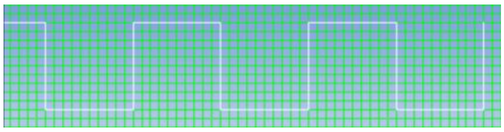

Figure 2. Excerpt of the mesh.

4. RESULTS AND DISCUSSION

Typical variations of the mean Nusselt numbers based on heat transfer rates averaged over the total surface area of the below plate and over the total surface area of the above plate, i.e., $\overline{\mathrm{Nu}}_{d\ (\mathrm{below,total})}$ and $\overline{\mathrm{Nu}}_{d\ (\mathrm{above,total})}$ with Rayleigh number for various values of the dimensionless vertical distance between the plates, *D*, and for various values of the dimensionless wave height, H, were obtained. Values of the dimensionless vertical distances that were used are 0.1, 0.3, 0.5, 0.7 and 0.9. Besides, values of the dimensionless wave heights that were used both for above and below plates, are 0.013158, 0.026316, 0.052632, 0.078948 and 0.105264. Both plates have unit depth w and unit width *L* maintained at a uniform surface temperature $T_w = 310$ K. The surrounding fluid is air at a temperature $T_f = 290$ K at atmospheric pressure. Numerical simulations were performed for Rayleigh numbers varying between 10^6 to 10^{12}.

In Figs. 3 to 7 are shown the variation of the mean total Nusselt number for the above/below wavy plates with the Rayleigh number for $B = H = 0.052632$ in the cases where $D = 0.1$, 0.3, 0.5, 0.7 and 0.9:

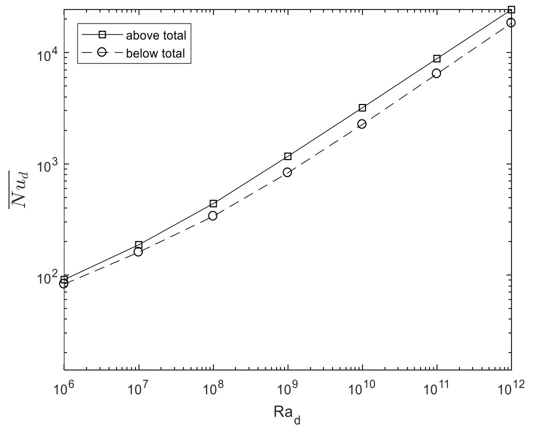

Figure 3. Variation of the mean total Nusselt number for the above/below wavy plates with the Rayleigh number for $B = H = 0.0526232$ and $D = 0.1$.

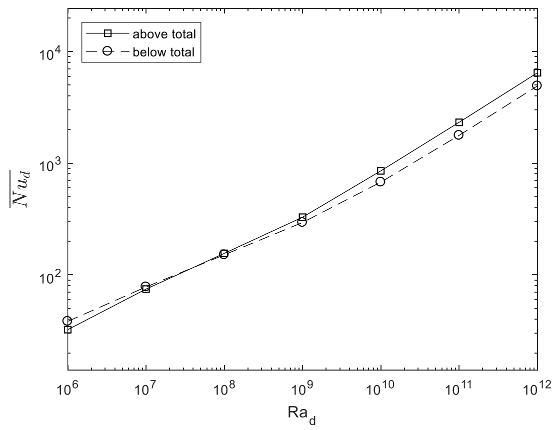

Figure 4. Variation of the mean total Nusselt number for the above/below wavy plates with the Rayleigh number for $B = H = 0.052632$ and $D = 0.3$.

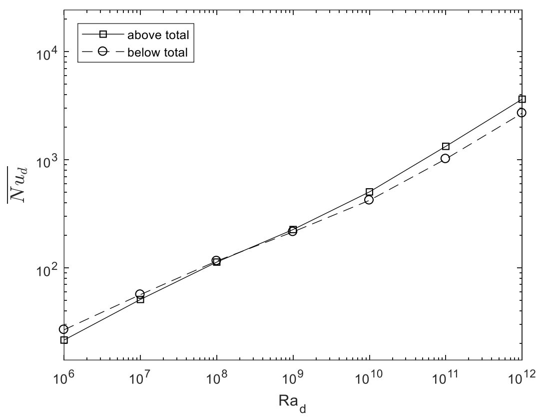

Figure 5. Variation of the mean total Nusselt number for the above/below wavy plates with the Rayleigh number for $B = H = 0.052632$ and $D = 0.5$.

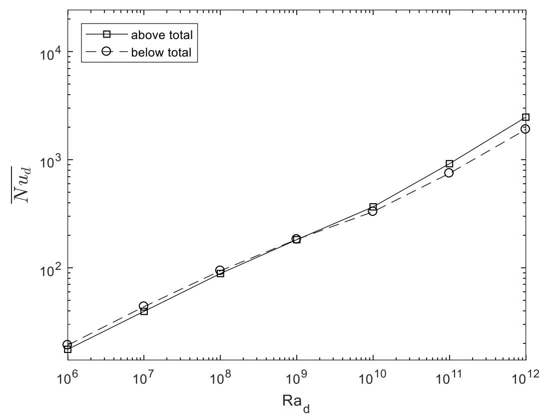

Figure 6. Variation of the mean total Nusselt number for the above/below wavy plates with the Rayleigh number for $B = H = 0.052632$ and $D = 0.7$.

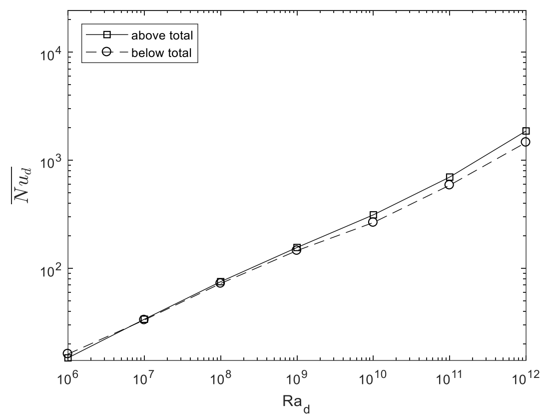

Figure 7. Variation of the mean total Nusselt number for the above/below wavy plates with the Rayleigh number for $B = H = 0.052632$ and $D = 0.9$.

In Figs 3 to 7, it can be seen a decrease in the mean total Nusselt number for both plates with an increase of the distance between the plates. Also, it can be noted that, in general, the mean total Nusselt number is bigger for the above plate than for the below plate, especially for high Rayleigh numbers. Moreover, the variation of the mean total Nusselt number between above and below plates decrease with an increase of *D*. In Fig 8, are shown the variation of the mean total Nusselt number for the above/below wavy plates with the dimensionless vertical distance between the plates for $B = H = 0.052632$ in the case where the Rayleigh numbers are equal to 10^6, 10^8, 10^{10} and 10^{12}.

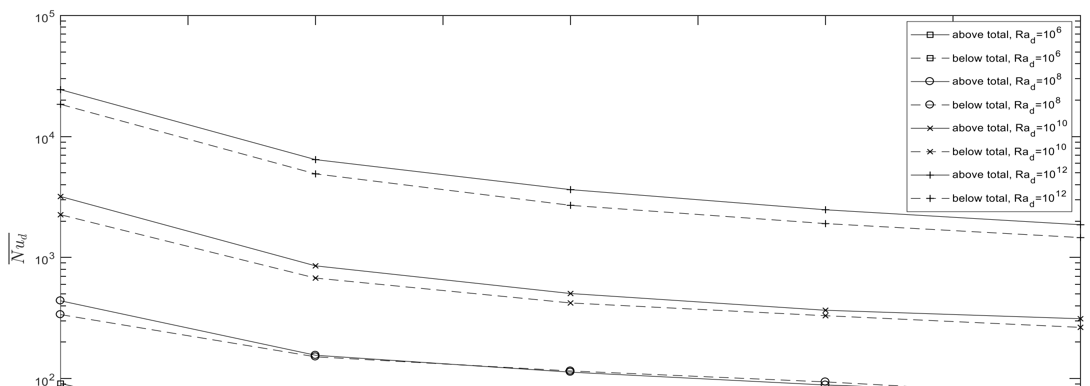

Figure 8. Variation of the mean total Nusselt number for the above/below wavy plates with the dimensionless vertical distance for $B = H = 0.052632$ for Rayleigh numbers equal to 10^6, 10^8, 10^{10} and 10^{12}

Figure 8 show another way to see the results of the Figs. 3 to 7. Again, it can be seen a decrease in the mean total Nusselt number for both plates with an increase of the dimensionless distance between the plates. Also, it can be noted that, in general, the mean total Nusselt number is bigger for the above plate than for the below plate, especially for high Rayleigh numbers. Moreover, the variation of the mean total Nusselt number between above and below plates decrease with an increase of *D*. Although these results have been placed in a graphical form for Rayleigh numbers equal to 10^6, 10^8, 10^{10} and 10^{12}, the same behavior was observed for Rayleigh numbers equal to 10^7, 10^9 and 10^{11}.

In Figs. 9 to 12, are shown the variation of the mean total Nusselt number for the above/below wavy plates with the Rayleigh number for $B = 0.052632$ and $D = 0.3$ in the cases where H = 0.013158, 0.026316, 0.052632, 0.078948 and 0.105264:

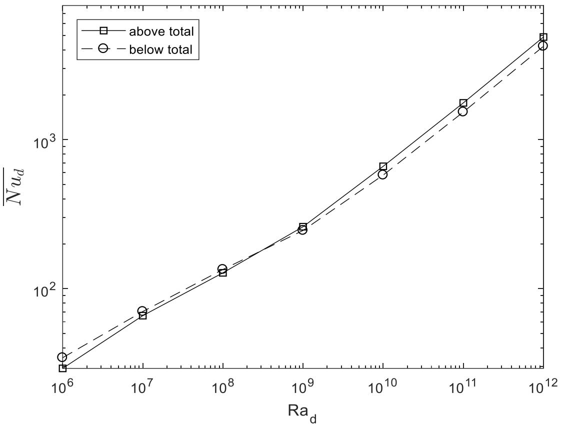

Figure 9. Variation of the mean total Nusselt number for the above/below wavy plates with the Rayleigh number for $B = 0.052632$, $H = 0.013158$ and $D = 0.3$.

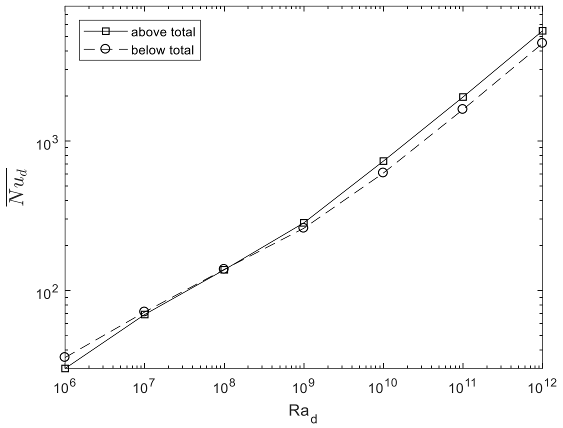

Figure 10. Variation of the mean total Nusselt number for the above/below wavy plates with the Rayleigh number for $B = 0.052632$, $H = 0.026316$ and $D = 0.3$.

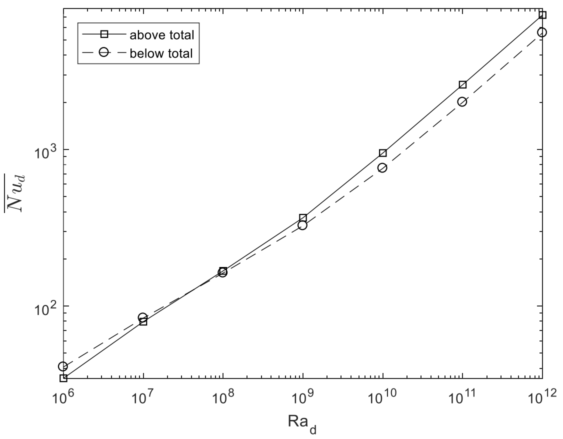

Figure 11. Variation of the mean total Nusselt number for the above/below wavy plates with the Rayleigh number for $B = 0.052632$, $H = 0.078947$ and $D = 0.3$.

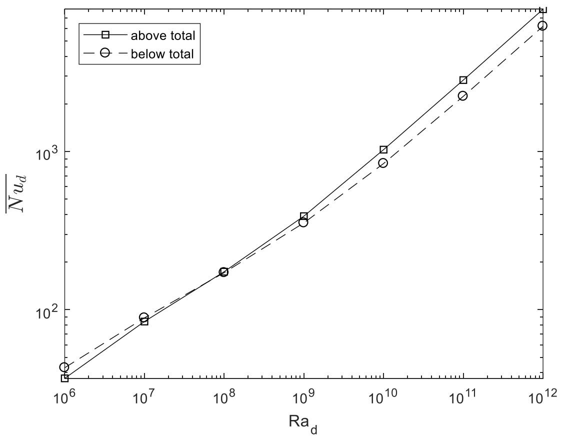

Figure 12. Variation of the mean total Nusselt number for the above/below wavy plates with the Rayleigh number for $B = 0.052632$, $H = 0.105264$ and $D = 0.3$.

In Figs. 9 to 12, it can be seen an increase in the mean total Nusselt number for above/below plates with the increase of *H*. Besides, it can be noted that the mean above total Nusselt number are lower than the mean below total Nusselt number up to approximately Rayleigh number equal of 10^8. From this value, an inverse behavior was observed. In Fig 13, are shown the variation of the mean total Nusselt number for the above/below wavy plates with the dimensionless height of the waves for $B = 0.052632$ and $D = 0.3$ in the case where the Rayleigh numbers are equal to 10^6, 10^8, 10^{10} and 10^{12}.

As expected, Fig. 13 show another way to see the results of the Figs. 9 to 12. Again, it can be seen an increase in the mean total Nusselt number for both plates with an increase of the dimensionless height of the waves. Also, it can be noted that, in general, the mean total Nusselt number is bigger for the above plate than for the below plate, especially for high Rayleigh numbers. Moreover, the variation of the mean total Nusselt number between above and below plates increase with an increase of *H*. Although these results have been placed in a graphical form for Rayleigh numbers equal to 10^6, 10^8, 10^{10} and 10^{12}, the same behavior was observed for Rayleigh numbers equal to 10^7, 10^9 and 10^{11}.

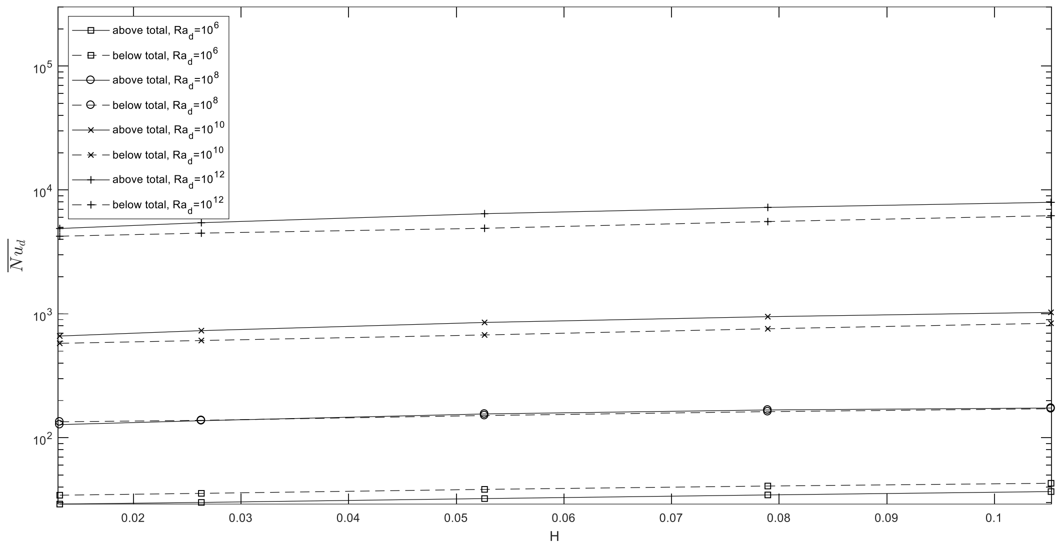

Figure 13. Variation of the mean total Nusselt number for the above/below wavy plates with the dimensionless wave height for $B = 0.052632,\ D = 0.3,\ \mathrm{Ra}_D = 10^6, 10^8, 10^{10}$ and 10^{12}.

In Fig. 13 are show an increase of up to 64% in the mean total Nusselt number for the above/below plates with an increase in the dimensionless height of the waves. The maximum percentual variation in mean total Nusselt number for the above/below wavy plates with the dimensionless wave height for $B = 0.052632$ and $D = 0.3$ can be seen in Tab. 2:

Table 2. Maximum percentual variation for the mean total Nusselt number for the above/below plates and for $B = 0.052632$ and $D = 0.3$.

Ra_d	$H = 0.013158$	$H = 0.026316$	$H = 0.052632$	$H = 0.078948$	$H = 0.105264$
10^6	15.20%	15.53%	15.73%	15.25%	14.31%
10^7	6.18%	3.79%	4.29%	5.13%	5.15%
10^8	5.07%	0.69%	3.01%	3.19%	1.39%
10^9	5.92%	8.69%	11.57%	12.44%	10.30%
10^{10}	14.53%	20.16%	26.16%	25.22%	22.43%
10^{11}	15.17%	21.15%	30.88%	29.62%	26.71%
10^{12}	15.37%	21.36%	31.15%	30.10%	28.21%

Besides, the maximum percentual variation in mean total Nusselt number for the above/below wavy plates with the dimensionless vertical distance between the plates for $B = H = 0.052632$ can be seen in Tab. 3:

Table 3. Maximum percentual variation for the mean total Nusselt number for the above/below plates and for $B = H = 0.052632$.

Ra_d	$D = 0.1$		$D = 0.3$		$D = 0.5$		$D = 0.7$		$D = 0.9$	
	ABOVE	BELOW	ABOVE	BELOW	ABOVE	BELOW	ABOVE	BELOW	ABOVE	BELOW
10^6	425.82%	-74.63%	75.96%	-67.53%	4.95%	-58.34%	-26.86%	-66.53%	-39.79%	-64.41%
10^7	465.34%	-52.68%	148.84%	-49.18%	39.63%	-36.40%	3.63%	-33.21%	-15.92%	-46.01%
10^8	378.05%	-39.42%	195.04%	-23.61%	82.03%	-9.18%	35.76%	-0.72%	13.98%	-13.35%
10^9	424.18%	-24.63%	145.84%	-11.59%	89.65%	15.18%	63.05%	31.77%	43.78%	19.15%
10^{10}	420.48%	-16.80%	143.05%	4.48%	84.39%	20.43%	58.59%	38.74%	34.51%	39.74%
10^{11}	408.79%	-14.39%	138.12%	17.88%	90.41%	41.45%	69.29%	61.10%	52.31%	67.12%
10^{12}	393.12%	-13.98%	127.06%	19.83%	85.95%	51.40%	69.62%	80.64%	57.30%	96.21%

It was observed that the Nusselt number had a higher incidence in the above plate, with greater concentration at the top for the distances $D = 0.1$, 0.3 and 0.5. In the distances $D = 0.7$ and 0.9 and lower Rayleigh values the Nusselt number had a higher concentration in the bottom. In the below plate, with distance $D = 0.1$, the highest incidence of

Nusselt Number was at the bottom of the plate, with distance $D = 0.3$ this is maintained for lower Rayleigh values ($Ra10^9$), in cases $D = 0.5$, 0.7 and 0.9 the number of Rayleigh had a higher incidence at the bottom for lower Rayleigh values ($Ra10^8$).

5. CONCLUSIONS

From the results of this work, it can be concluded that the vertical distance between the plates interferes directly in the mean total Nusselt number for the above and below plates. With plates closer, the mean total Nusselt number is higher on the above plate, with the distance between the above and below plates, the mean total Nusselt number decrease in both plates and the variation of the mean total Nusselt number tends to alternate between the above and below plates. For low Rayleigh values, the mean total Nusselt number is higher for the below plate and for high Rayleigh values, the higher concentration on the above plate. The increase in the surface area also increases the mean total Nusselt number, being larger the area greater the mean total Nusselt number both on the above and below plates. This behavior shows interference between the plates, because the greater the area of surface, the greater was the variation in the mean total Nusselt number between the above and below plate.

6. REFERENCES

Oliveira, S.D.R. and Oosthuizen, P.H., 2018. "A numerical study of the simultaneous natural convective heat transfer from the top and bottom surfaces of a thin horizontal plane having a wavy surface". In *26th Annual Conference of the Computational Fluid Dynamics Society of Canada* – CFD 2018, Winnipeg, Canada.

Oliveira, S.D.R. and Oosthuizen, P.H., 2019. "A numerical study of the simultaneous natural convective heat transfer from the top and bottom surfaces of a thin inclined plate having a wavy surface with constant height". In *4th Thermal and Fluids Engineering Conference* – TFEC 2019, Las Vegas, USA.

Oosthuizen, P.H., 2016. "External natural convective heat transfer from bodies having a wavy surface for conditions under which laminar, transitional, and turbulent flow can exist". *Advances in Heat Transfer*, Vol. 48, p. 261-317.

Oosthuizen, P.H., 2016a. "A numerical study of natural convective heat transfer from a horizontal isothermal surface with rectangular surface roughness elements". In *Proceedings of the First Pacific Rim Thermal Engineering Conference* – PRTEC 2016, Hawaii's Big Island, USA.

Oosthuizen, P.H., 2016b. "A numerical study of the effect of triangular waves on natural convective heat transfer from an upward facing heated horizontal isothermal surface". In *ASME 2016 International Mechanical Engineering Congress and Exposition*, Phoenix, USA.

Prétot, S., Zeghmati, B. and Caminat, Ph., 2000. "Influence of surface roughness on natural convection above a horizontal plate". *Advances in Engineering Software*, Vol. 30, p. 793-801.

Prétot, S., Miriel, J., Baily, Y. and Zeghmati, B., 2003. "Visualization and simulation of the natural convection flow above horizontal wavy plates". *Numerical Heat Transfer, Part A: Applications*, Vol. 43, p. 307-325.

Siddiqa, S. and Hossain, M.A., 2013. "Natural convection flow over wavy horizontal surface". *Advances in Mechanical Engineering*, Vol. 5, p. 1-7.

Schmidt, R. C. and Patankar, S. V., 1991. "Simulating boundary layer transition with low-Reynolds-Number *k-ε* turbulence models: Part 1- an evaluation of prediction characteristics". *ASME Journal of Turbomachinery*, Vol. 113, p. 10-17.

Siddiqa, S., Hossain, M.A. and Gorla, R.S.R., 2015. "Natural convection flow of viscous fluid over triangular wavy horizontal surface". *Computers & Fluids*, Vol. 5, p. 130-134.

Zheng, X., Liu, C., Liu, F. and C.-I. Yang., 1998. "Turbulent transition simulation using the *k-ω* model". *International Journal for Numerical Methods in Engineering*, Vol. 42, p. 907-926.

7. RESPONSIBILITY NOTICE

The authors are the only responsible for the printed material included in this paper.